Asian Journal of Chemistry; Vol. 25, No. 6 (2013), 3023-3029

ASIAN JOURNAL OF CHEMISTRY

http://dx.doi.org/10.14233/ajchem.2013.13496

Study on Fingerprints of Different Organs of *Arabidopsis thaliana* by Using UPLC/ESI-Q-TOF MS

HONGZHI ZHAO[1], JING WANG[1], CHUNFENG XIE[1], SHENGYOU SONG[1], GANG BAI[1,*] and GUOAN LUO[1,2,*]

[1]College of Pharmacy, Nankai University, Tianjin 300071, P.R. China
[2]Department of Chemistry, Tsinghua University, Beijing 100084, P.R. China

*Corresponding authors: Tel/Fax: +86 22 23506792; +86 10 62781688; E-mail: gangbai@nankai.edu.cn; luoga@nankai.edu.cn

(*Received*: 23 January 2012; *Accepted*: 10 December 2012) AJC-12511

To investigate the fingerprint of *A. thaliana* and compare those of the four different organs (rosette leaves, stems, flowers and stem leaves), an ultra performance liquid chromatography coupled with electrospray ionization quadrupole/time of flight mass spectrometry (UPLC/ESI-Q-TOF MS) was employed. Compounds were separated on the C_{18} column using a gradient elution of acetonitrile and 0.1 % formic acid in water. The principal components analysis was applied for data treatment. Clear discrimination was obtained in the score plot, providing the difference in chemical characteristic of different organs. Twenty compounds including flavone glycosides, oxylipins, aliphatic acids and others were identified based on their high resolution mass spectra and the MS/MS fragmentation pathways. It is concluded that the several compounds (oxophytodienoid acid, sn-2-O-(dinoroxophytodienoyl) monogalactosyl monoglyceride, kaempferitrin, robinin, arabidopside E and arabidopside A) were significant markers in the different organs of *A. thaliana*.

Key Words: *Arabidopsis thaliana*, Fingerprint, UPLC/Q-TOF mass spectrometry, Principal components analysis.

INTRODUCTION

LC-MS analysis combined with multivariate data analysis was an effective method for the fingerprinting study on plant. Arbona *et al.*[1] demarcated five plant phenotypes (*Arabidopsis, Prunus*, citrumelo, Cleopatra and Carrizo) using LC-MS and GC-MS combined with principal components analysis and hierarchical clustering analysis.

Arabidopsis thaliana is a model plant. The leaves form a rosette at the base of the plant, with a few leaves also on the flowering stem. Many secondary metabolites, such as oxylipins, flavonoids, sinapoyl derivatives, glucosinolates and pigments were reported in *A. thaliana*[2]. Stobiecki *et al.*[3] identified and quantified the phenolic glycosidic conjugates and flavonoid conjugates isolated from *A. thaliana* leaves by LC/MS. Some of the researches on *A. thaliana* focused on the rosette leaf tissue. For example, Fiehn *et al.*[4] identified more than 15 uncommon plant metabolites in polar fractions of *A. thaliana* leaf extracts, such as tartronate semialdehyde, citramalic acid, allothreonine, or glycolic amide. Rosette leaf tissue of *A. thaliana* was studied for the search of new metabolites involved in wound signaling[5]. Some researchers combined all of aerial parts of *A. thaliana* to obtain the fingerprint ignoring the differences of different organs[6,7]. However, each organ has a dedicated metabolism in order to perform effectively its desired function[8] and they may have some differences in their fingerprints. The fingerprints in different organs need to be obtained respectively.

In this study, fingerprints of different organs (rosette leaves, stems, flowers and stem leaves) of *A. thaliana* were obtained using ultra-performance liquid chromatography-quadrupole-time-of-flight mass spectrometry (UPLC/Q-TOF MS), which was widely used due to its high speed, sensitivity and specificity in recent years[9,10]. The data were treated by taking the advantage of both chromatographic information and accurate mass determination. Multivariate analysis method principal components analysis was used. The study of significant metabolite variation related to different organs in *A. thaliana* was investigated for a relatively large number of plant specimens. This technique can be recently applied for other plants and potentially elucidate the mechanism of inherent phytochemical diversity.

EXPERIMENTAL

Acetonitrile for LC and MS analysis was of LC grade from Fisher (USA); formic acid for MS analysis was LC grade from (Acros, USA); water for LC and MS analysis was purified by a Milli-Q academic water purification system (Millipore, Milford, MA, USA).

A. thaliana (ecotype Columbia-0) was grown in a controlled environment and maintained under the condition of an average temperature of 22 ºC, 70 % relative humidity and a

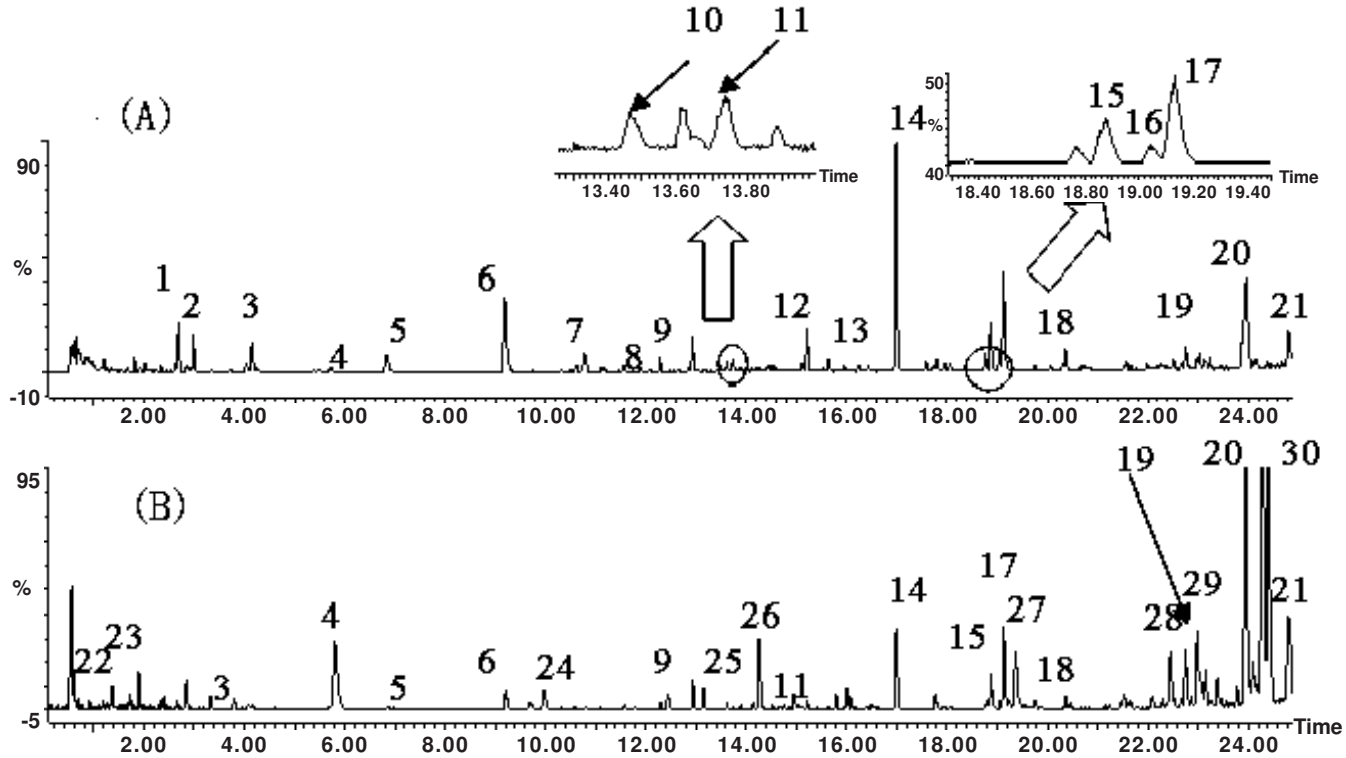

Fig. 1. Base-peak intensity chromatograms of rosette leaf obtained by UPLC/TOF MS; (A) negative-ion mode (B) positive-ion mode

day length of 16 h, containing 12 individual plants. After 30 days, rosette leaves, stems, flowers and stem leaves were harvested respectively and immediately frozen in liquid nitrogen and then placed in a -80 ºC freezer until extraction (n = 12).

Sample preparation: Plant material was ground in a mortar with liquid nitrogen. Approximately 100 mg of tissues were extracted with 1 mL MeOH-H_2O (80:20, v/v). The extracts were centrifuged for 15 min (4 ºC, 13000 rpm). Supernatant was isolated and maintained at -20 ºC until LC-MS analysis.

UPLC conditions: The separations were carried out on waters Acquity UPLC BEH C_{18} column (2.1 mm × 100 mm, 1.7 μm) at 30 ºC. The mobile phase consisted of acetonitrile as solvent A and 0.1 % formic acid in water as solvent B. Separation was performed by gradient elution as shown in Table-1. The injection volume of the test sample was 2 μL. Every sample was injected three times.

TABLE-1
SOLVENT COMPOSITION OF THE GRADIENT OF THE UPLC ANALYSIS

Time (min)	A (%)	B (%)	Curve
Initial	2	98	Initial
2	12	88	Linear
8	15	85	Linear
17	60	40	Linear
26	100	0	Linear

A is acetonitrile and B is 0.1 % aqueous formic acid solution

Mass spectrometry conditions: Mass spectrometry was carried out on a Waters Q-TOF premier with electrospray ionization system (Waters MS Technologies, Manchester, UK). The ESI-MS spectra were acquired in both negative and positive-ion modes. The conditions of ESI-MS analysis were as follows: The capillary voltage was set to 2.5 kV for negative and 3.0 kV for positive-ion mode and the sample cone voltage was 30 V. The desolvation gas flow was set to 600 L/h at a desolvation temperature of 300 ºC, the cone gas set to 50 L/h and the source temperature was 100 ºC. MS spectra are acquired from 50 till 1500 Da. MS/MS experiments were conducted by setting the Q-TOF Premier quadrupole to allow ions of interest to pass before fragmentation in the collision cell with argon as collision gas for generation of abundant product ions before detection in the TOF analyzer.

Data analysis: Data preprocessing was performed with MassLynx applications manager version 4.1 (Waters, MA, USA). Principal components analysis was performed using MarkerLynx software (Waters, MA, USA).

RESULTS AND DISCUSSION

Optimization of a UPLC/TOF MS fingerprint method: Different extraction solvents were investigated, such as MeOH-H_2O (50:50, v/v), MeOH-H_2O (80:20, v/v) and MeOH. MeOH-H_2O (80:20, v/v) was selected finally. This solvent provided was suitable for extracting the components in plant[11]. The UPLC chromatographic conditions were optimized for analyzing speed and sensitivity, with special emphasis on the good separation resolution. High-resolution mass spectra (HRMS) were performed on a waters Q-TOF Premier mass spectrometer. Capillary voltage, source temperature and desolvation temperature were important parameters in TOF MS analysis. After a series of optimization, the conditions for mass spectrometry employed can be used as expressed as mentioned above. The classical base-peak intensity (BPI) chromatograms in negative-ion and positive-ion modes of rosette leaf were shown in Fig. 1.

Validation of the method: The fingerprint analysis is not a quantitative method. The parameters evaluated and validation aspects are different from assaying methods. Intra- and inter-day precision of the method were determined. The intra-day variability evaluation was performed six times on the same sample during a single day, while the inter-day precision evaluation was carried out in triplicate on another independent sample on three different days. The RSD of relative retention time and relative peak area were below 3 %. The test precision of sample stability was determined with one sample during 24 h. During this period, the solution was stored at room temperature. The RSD of relative retention time and relative peak area were below 3 %. It was indicated that the sample remained stable during this period.

Identification of the compounds: The deprotonated $[M-H]^-$ and protonated $[M+H]^+$ molecules were selected as precursor ions for fragmentation to produce MS/MS product-ion spectra. The results are listed in Table-2. Based on the high resolution mass spectrum and their MS/MS fragmentation pathways, 20 compounds were identified belonging to flavonoids, oxylipins and other classes.

Flavones are a class of plant secondary metabolites bearing a skeleton of 2-phenylchromen-4-one (2-phenyl-1-benzopyran-4-one). Compounds **2, 3, 4, 5, 6, 16, 19** were identified to be flavonoid derivatives, based on the MS/MS information and reported literatures[3,12,13]. As shown in Fig. 2A, one of the ions set was the $[M-H]^-$ ion *m/z* 739, eluting with a retention time (RT) of 4.15 min in the UPLC separation. Its molecular formula was presumed to be $C_{33}H_{40}O_{19}$ from the $[M-H]^-$ ion peak at 739 and $[M+H]^+$ ion peak at 741 in the high-resolution MS (HR MS). The ions *m/z* 739 and 741 were selected as the precursor ions in the negative and positive-ion modes MS/MS spectrum respectively. As shown in the MS/MS spectra (Fig. 2), the fragments $[M-H-146]^-$, $[M-H-309]^-$, $[M-H-146-309]^-$, $[M+H-146]^+$, $[M+H-308]^+$, $[M+H-146]^+$, $[M+H-146-308]^+$ were observed. The cleavage result was in agreement with that of robinin reported in the literature[14]. This component was identified as robinin (kaempferol-3-O-rhamnosyl-glucoside-7-O-rhamnoside, compound **3**). The molecular formula was $C_{33}H_{40}O_{19}$. It has been identified previously from *A. thaliana*[15].

Another ion identified from the loading plot as being responsible for the variance in the data set was the $[M-H]^-$ ion *m/z* 577, eluting with a RT of 9.20 min in the UPLC separation. The peak of *m/z* 579 was observed at the same retention time in the chromatography of positive-ion mode. The ions *m/z* 577 in negative-ion mode and *m/z* 579 in positive-ion mode were $[M-H]^-$ and $[M+H]^+$, respectively. Thus the molecular weight was presumed to be 578. In negative-ion mode, the MS/MS spectrum (Fig. 3A) contained an abundant ion formed by loss of 146 Da ($C_6H_{10}O_4$), forming the ions $[M-H-146]^-$ and $[M-H-146-146]^-$, at *m/z* 431 and 285 respectively. While in positive-ion mode, the MS/MS spectrum (Fig. 3B) contained an abundant ion formed by loss of 146 Da ($C_6H_{10}O_4$), forming the ions $[M+H-146]^+$ and $[M+H-146-146]^+$, at *m/z* 433 and 287 respectively. This compound was identified as kaempferitrin (kaempferol 3,7-bisrhamnoside, compound **6**). The MS/MS data was in good agreement with the literature[16].

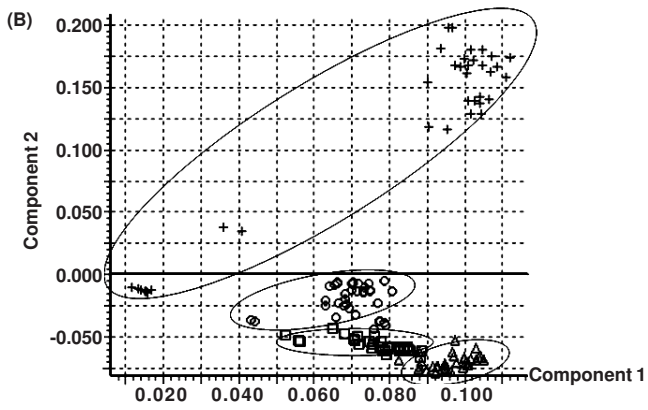

Fig. 2. Scores plot (A) negative-ion mode (B) positive-ion mode; (□ stem + rosette leaf; Δ flower ○ stem leaf)

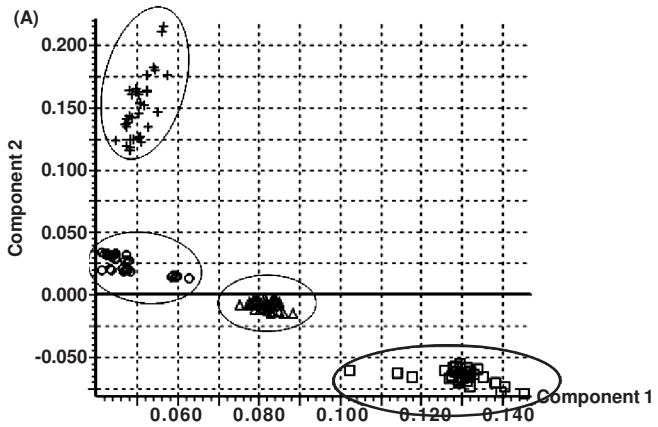

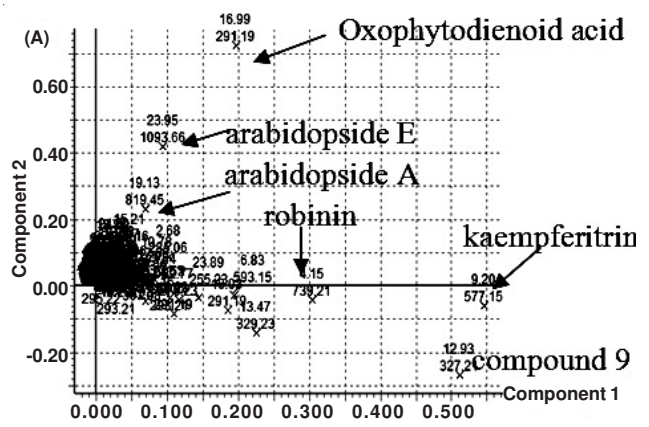

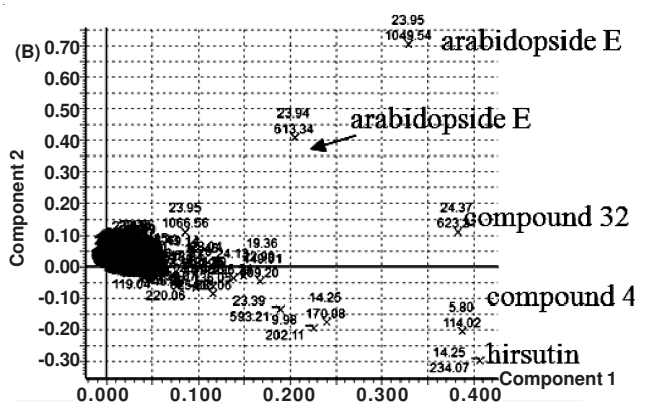

Fig. 3. Loading plot: (A) negative-ion mode (B) positive-ion mode

TABLE-2
IDENTIFICATION OF THE COMPOUNDS AND ITS SIGNIFICANCE OF PRINCIPAL COMPONENTS ANALYSIS

Comp.	Retention time	MS (*m/z*)	Significance	MS/MS fragment (*m/z*)	Identity	m.f.	m.w.	Substance Class
1	2.67	(-) 285	(-) 0.0960	(-) 153, 109	Unknown	/	/	/
2	2.99	447 $[M-H]^-$	(-) 0.0038	(-) 285	Kaempferol 3-*O*-glucoside	$C_{21}H_{20}O_{11}$	448.1006	Flavone glycoside
3	4.15	739 $[M-H]^-$	(-) 0.2162	(-) 593, 430, 284, 180	Robinin	$C_{33}H_{40}O_{19}$	740.2164	Flavone glycoside
		741 $[M+H]^+$	(+) 0.0025	(+) 595, 433, 287				
4	5.80	(-) 431	/	(-) 385	Unknown	/	/	/
		(+) 387	(+) 0.2193	(+) 178, 114				
5	6.82	593 $[M-H]^-$	(-) 0.1382	(-) 447, 431, 285	Kaempferol 3-*O*-glucoside 7-*O*-rhamnosidea	$C_{27}H_{30}O_{15}$	594.1585	Flavone glycoside
		595 $[M+H]^+$	(+) 0.0013	(+) 433, 287				
6	9.20	577$[M-H]^-$	(-) 0.3877	(-) 430, 285,	Kaempferitrin	$C_{27}H_{30}O_{14}$	578.1636	Flavone glycoside
		579$[M+H]^+$	(+) 0.0191	(+) 433, 287				
7	10.79	(-) 403	(-) 0.0459	(-) 97	Unknown	/	/	/
8	12.28	707$[M-H+HCOOH]^-$ 661$[M-H]^-$	(-) 0.0261	(-) 415, 263, 397	Sn2-*O*-(dinor-oxophytodienoyl)-digalactosyl monogylceride	$C_{31}H_{50}O_{15}$	662.3150	Oxylipin
9	12.93	545$[M-H+HCOOH]^-$ 499 $[M-H]^-$	(-) 0.4071	(-) 327, 263, 253, 245	Sn2-*O*-(dinor-oxophytodienoyl)-monogalactosyl monogylceride	$C_{25}H_{40}O_{10}$	500.2621	Oxylipin
		501 $[M+H]^+$	(+) 0.0001	(+) 339, 321, 265, 247				
10	13.47	329 $[M-H]^-$	(-) 0.1877	(-) 229, 211, 156	9,12,13-trihydroxy-10(E)-octadecenoic acid	$C_{18}H_{34}O_5$	330.2406	Aliphatic acid
11	13.74	325 $[M-H]^-$	(-) 0.0323	(-) 307, 237,116	butanedioic acid	$C_{14}H_{14}O_9$	326.0638	Other
12	15.21	263 $[M-H]^-$	(-) 0.0927	(-) 245,219	Abscisic acid	$C_{15}H_{20}O_4$	264.1362	Sesquiterpene
		265 $[M+H]^+$	(+) 0.0094	(+) 247, 229, 219, 201				
13	15.64	(-) 309	(-) 0.0366	(-) 309, 265, 209, 152	Unknown	/	/	/
14	16.99	291.2$[M-H]^-$	(-) 0.5306	(-) 247$[M-H-CO_2]^-$, 165$[M-H-CO_2-C_6H_9]^-$	Oxophytodienoic acid (OPDA)	$C_{18}H_{28}O_3$	292.2038	Aliphatic acid
		315 $[M+Na]^+$, 293 $[M+H]^+$,	(+) 0.0920	(+) 275 $[M+H-H_2O]^+$, 257$[M+H-H_2O]^+$				
15	18.86	(-)1009.5 $[M-H+HCOOH]^-$, 963$[M-H]^-$	(-) 0.0771	(-) 871, 689, 671, 397, 291	Arabidopsides D	$C_{51}H_{80}O_{17}$	964.5396	Oxylipin
		(+) 965$[M+H]^+$	(+) 0.0043	(+) 641, 623, 349, 275				
16	19.05	(-) 431$[M-H]^-$	(-) 0.1045	(-) 285,151	Kaempferol rhamnoside	$C_{21}H_{20}O_{10}$	432.1056	Flavone glycoside
17	19.13	819.5 $[M-H+HCOOH]^-$, 773 $[M-H]^-$	(-) 0.1711	(-) 291, 263, 253, 245	Arabidopside A	$C_{43}H_{66}O_{12}$	774.4554	Oxylipin
18	20.36	847$[M-H+HCOOH]^-$ 801$[M-H]^-$	(-) 0.0391	(-) 847, 801, 527, 291, 253	Arabidopside B	$C_{45}H_{70}O_{12}$	802.4867	Oxylipin
		825$[M+Na]^+$ 803$[M+H]^+$	(+) 0.0001	(+) 803, 641.4, 623.4				
19	22.76	(-) 995.5	(-) 0.0874	(-) 279,116	Unknown	/	/	/
		(+) 641	(+) 0.0008	(+) 623, 349, 293, 275, 257				
20	23.95	1093.6 $[M-H+HCOOH]^-$ 1047.6 $[M-H]^-$	(-) 0.3047	(-) 801, 527, 291, 263, 245	Arabidopside E	$C_{61}H_{92}O_{14}$	1048.6487	Oxylipin
		1049.5 $[M+H]^+$	(+) 0.5844	(+) 613, 595, 349, 321, 293, 275				
21	24.80	1121.7 $[M-H+HCOOH]^-$ 1075.7$[M-H]^-$	(-) 0.0795	(-) 801.5, 291.2	Arabidopside G	$C_{63}H_{96}O_{14}$	1076.6800	Oxylipin
22	1.37	(+) 268	(+) 0.0409	(+) 136	Adenosine	$C_{10}H_{13}N_5O_4$	267.0968	Other
23	1.99	(+) 120	(+) 0.0762	(+) 103, 91, 77	Threonine	$C_4H_9NO_3$	119.0582	Other
24	9.98	(+) 202	(+) 0.1752	(+) 138	Unknown	/	/	/
25	13.16	(+) 220,156	(+) 0.0885	(+) 156, 112, 122, 84	Unknown	/	/	/
26	14.26	234 $[M+H]^+$	(+) 0.3856	(+) 170	Hirsutin	$C_{10}H_{19}NOS_2$	233.0908	Isothiocyanate
27	19.36	(+) 643	(+) 0.0878	(-) 583, 555, 495, 443	Unknown	/	/	/
28	22.45	(+) 609	(+) 0.0505	(+) 591, 559, 531	Unknown	/	/	/
29	22.99	1241 $[2M+H]^+$ 621 $[M+H]^+$	(+) 0.1130	(-) 621, 593, 561, 533	Methyl phaeophorbide-b	$C_{36}H_{36}N_4O_6$	620.2635	Other
30	24.37	(+) 680	(+) 0.3205	(+) 680, 662, 630, 603, 575	Unknown	/	/	/

(+) Positive ion mode; (–) Negative ion mode

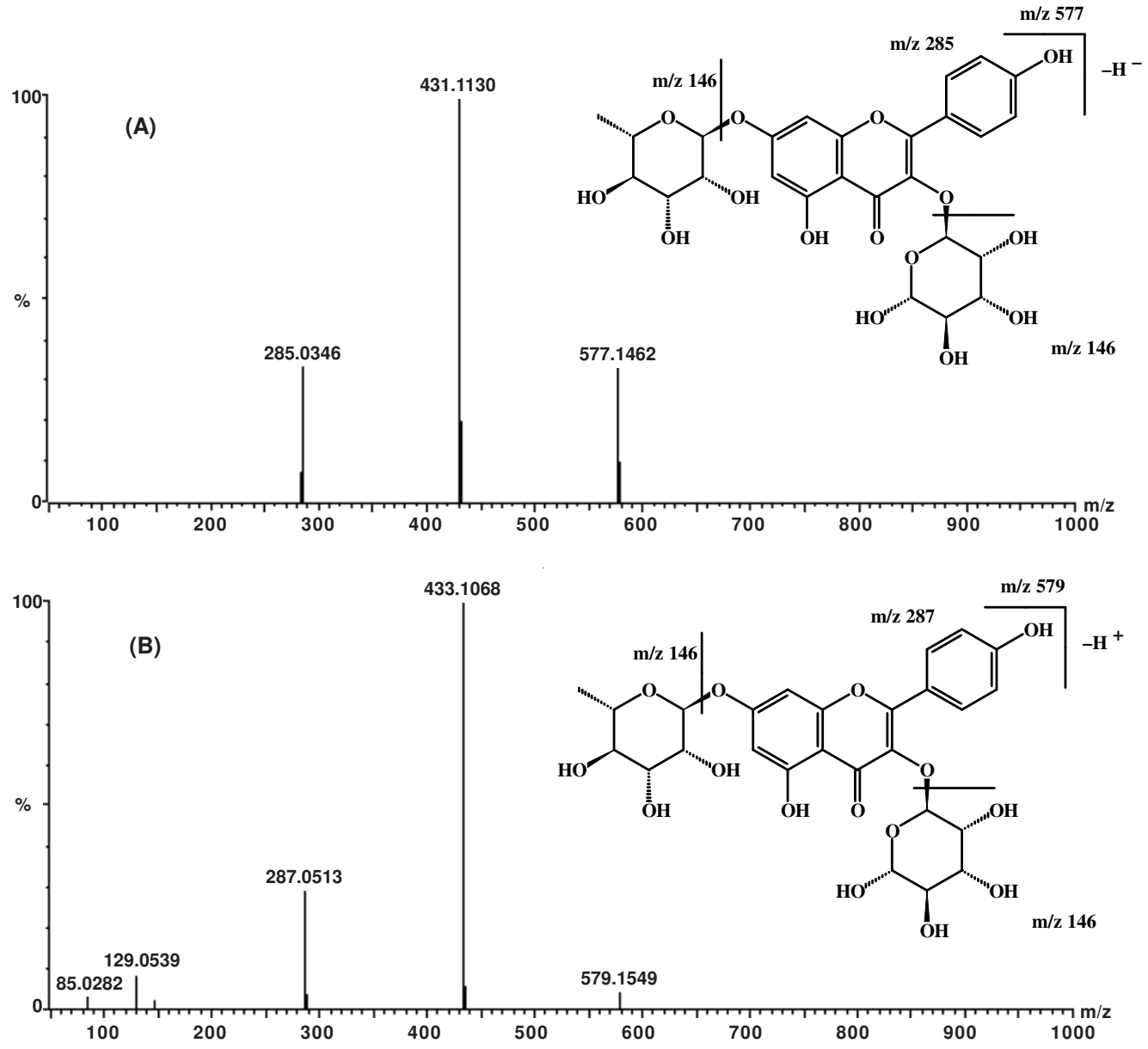

Fig. 4. MS/MS spectra in negative (A) and positive-ion mode (B) of compound **3**

Oxylipins (oxygenated fatty acid-derivatives) are central players in a variety of physiological processes in plants[17]. They originate from oxidation and further conversions of poly-unsaturated fatty acids, predominantly linoleic acid and linolenic acid[18].

The fragment ion *m/z* 291 was observed in compounds **14, 15, 17, 18, 20** and **21**. All the six compounds may have the similar fragment pathway. Based on the MS/MS information, they were identified to be oxophytodienoic acid, arabidopsides D, A, B, E and G, respectively. They all belong to oxylipins. As an example, compound **17** exhibited a $[M-H+HCOOH]^-$ ion at *m/z* 819.4516 ($C_{44}H_{67}O_{14}$, calculation mass 819.4531, error 1.8 ppm) and a $[M-H]^-$ ion at *m/z* 773.4233($C_{43}H_{66}O_{12}$, calculation mass 773.4476, error 31.4 ppm) with RT of 19.13 min in the UPLC separation. The fragment ion *m/z* 819 selected as precursor ions for fragmentation to produce MS/MS product-ion spectra. In the MS/MS spectrum (Fig. 4) of *m/z* 819, the fragment ions *m/z* 291.1965 oxophytodienoic acid ($C_{18}H_{27}O_3$, calculation mass 291.1960, error 1.7 ppm), *m/z* 263.1686 dn-OPDA ($C_{16}H_{23}O_3$, calculation mass 263.1647, error 14.8 ppm) were observed. This fragment result matched well with the data reported in the literature[19]. Consequently, compound **17** was determined as arabidopside A ($C_{43}H_{66}O_{12}$), which is a monogalactosyl diacylglyceride containing oxophytodienoic acid (OPDA, molecular formula $C_{18}H_{28}O_3$) and dinor-oxophytodienoic acid (dn-OPDA, molecular formula $C_{16}H_{24}O_3$).

Principal components analysis: Principal components analysis is a general tool for interpretation of large data tables[20,21]. In this study, the principal components analysis was used to distinguish different organs based on the fingerprints in both negative and positive-ion modes sequentially. It was carried out by the MarkerLynx software.

The principal components analysis score plots were displayed in Fig. 5. The clear discrimination of different organs of *A. thaliana* was observed in the Principal components analysis

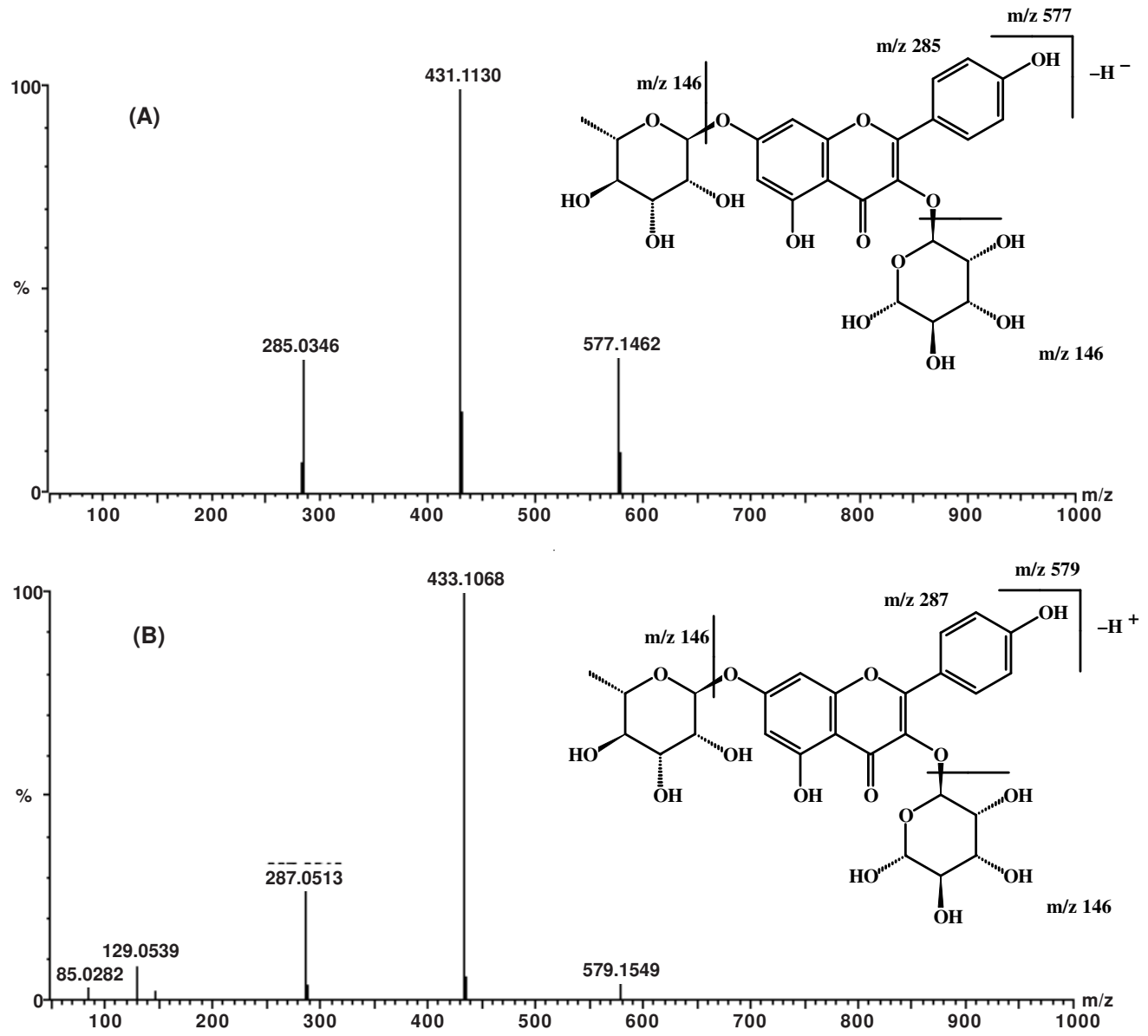

Fig. 5. MS/MS spectra in negative (A) and positive-ion mode (B) of compound **6**

scores plot where each coordinate represented a sample group. All the samples could be classified into four clusters (rosette leaves, stems, flowers and stem leaves). There was no any misclassification of these four groups.

Loading plots (Fig. 6) described how much each variable contributes to each principal component. The distance of the marker from the origin of the loadings plot scaled to a value between 0 and 1 and the significance was shown in Table-2. The higher the value was, the more significant the marker was. The ions responsible for the clustering were clearly visible with the compounds oxophytodienoic acid, sn2-O-(dinor-oxophytodienoyl)-monogalactosyl monogylceride and kaempferitrin, arabidopside B, robinin (Fig. 6A) contributing strongly to the clustering. Their significances (Table-2) were 0.5306, 0.4071, 0.3877, 0.3047 and 0.2162, respectively. On the other hand, the Principal components analysis loading plots (Fig. 6B) suggested many markers responsible for positive-ion mode fingerprint differences. Their significances (Table-2) were 0.5844 (arabidopside E), 0.3856 (hirsutin) and 0.3205 (compound **30**), respectively. As shown in Fig. 7, the base-peak intensity (BPI) chromatograms were significantly different for different organs of *A. thaliana*.

Conclusion

In this study, a UPLC/Q-TOF MS strategy was developed for the detection and localization of metabolites of different

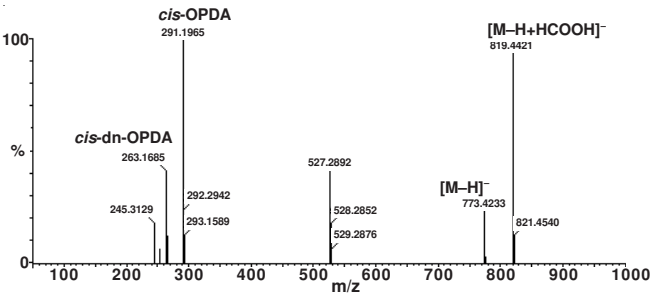

Fig. 6. MS/MS spectra in negative-ion mode of compound **17**

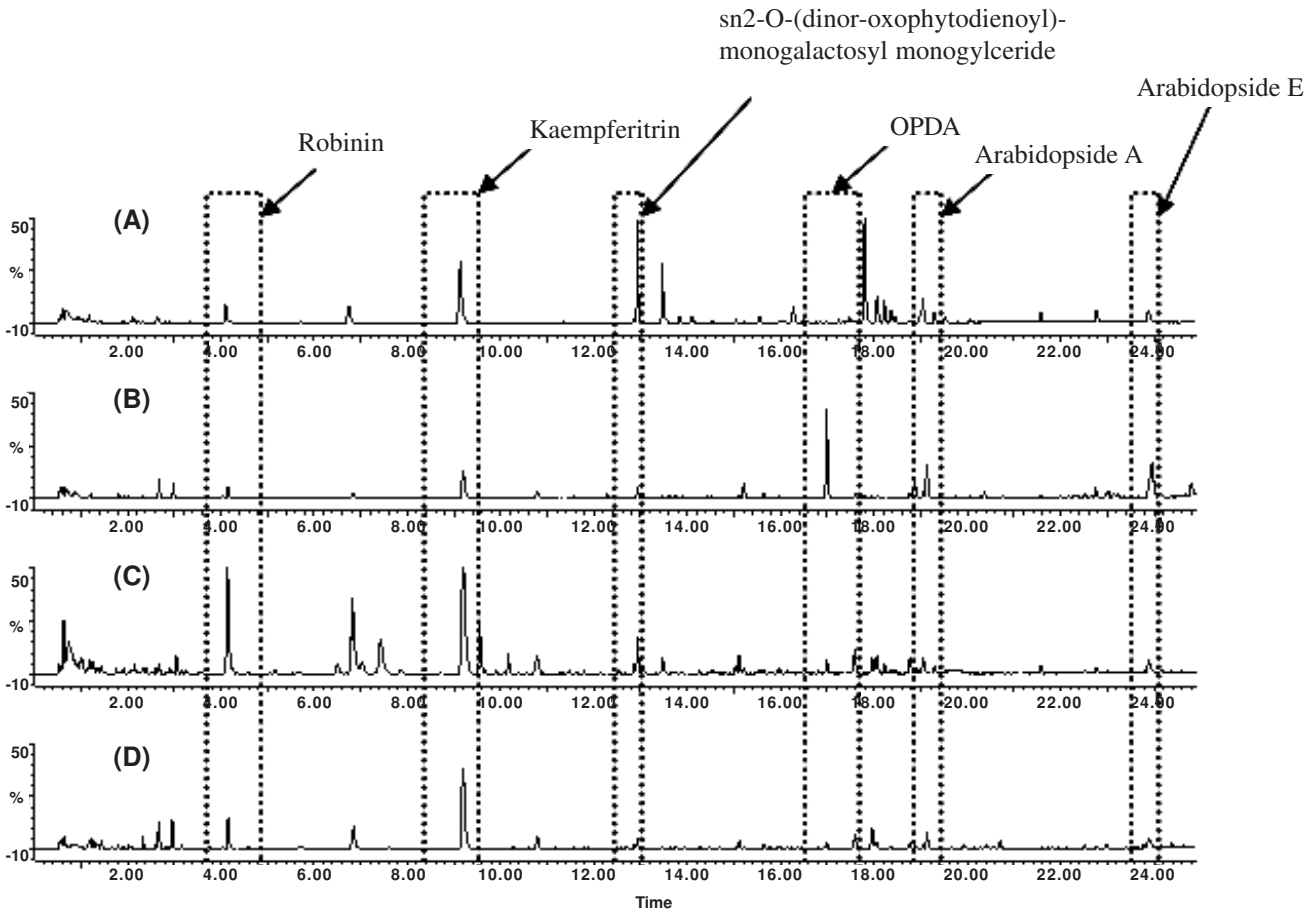

Fig. 7. BPI Chromatograms obtained by UPLC/TOF in negative-ion mode (A) stem (B) rosette leaf (C) flower (D) stem leaf

organs in *A. thaliana*. Based on the fingerprints in conjunction with principal components analysis, different organs samples were accurately discriminated. Twenty compounds were identified base on the high resolution mass spectrum and their fragmentation pathways. Among them, kaempferitrin, robinin, arabidopside E and arabidopside A were significant in the different organs of *A. thaliana*. The result laid a good foundation for our further research on plant physiology and biochemistry.

ACKNOWLEDGEMENTS

This study was supported by Major Program of National Natural Science Foundation of China (No. 90917003).

REFERENCES

1. V. Arbona, D.J. Iglesias, M. Talon and A. Gomez-Cadenas, *J. Agric. Food Chem.*, **57**, 7338 (2009).
2. E. Grata, J. Boccard, G. Glauser, P.A. Carrupt, E.E. Farmer, J.L. Wolfender and S. Rudaz, *J. Sep. Sci.*, **30**, 2268 (2007).
3. M. Stobiecki, A. Skirycz, L. Kerhoas, P. Kachlicki, D. Muth, J. Einhorn and B. Mueller-Roeber, *Metabolomics*, **2**, 197 (2006).
4. O. Fiehn, J. Kopka, R.N. Trethewey and L. Willmitzer, *Anal. Chem.*, **72**, 3573 (2000).
5. E. Grata, J. Boccard, D. Guillarme, G. Glauser, P.A. Carrupt, E.E. Farmer, J.L. Wolfender and S. Rudaz, *J. Chromatogr. B*, **871**, 261 (2008).
6. A. Fukushima, M. Kusano, H. Redestig, M. Arita and K. Saito, *BMC Syst. Biol.,* **5**, 1 (2011).
7. J.L. Ward, C. Harris, J. Lewis and M.H. Beale, *Phytochemistry*, **62**, 949 (2003).
8. R.D. Hall, *New Phytol*., **169**, 453 (2006).
9. I.S. Lurie and S.G. Toske, *J. Chromatogr. A*, **1188**, 322 (2008).
10. R.S. Plumb, M.D. Jones, P.D. Rainville and J.K. Nicholson, *J. Chromatogr. Sci.*, **46**, 193 (2008).
11. R.t'Kindt, L. De Veylder, M. Storme, D. Deforce and J. Van Bocxlaer, *J. Chromatogr. B*, **871**, 37 (2008).
12. P. Kachlicki, J. Einhorn, D. Muth, L. Kerhoas and M. Stobiecki, *J. Mass Spectrom.*, **43**, 572 (2008).
13 R. Nakabayashi, M. Kusano, M. Kobayashi, T. Tohge, K. Yonekura-Sakakibara, N. Kogure, M. Yamazaki, M. Kitajima, K. Saito and H. Takayama, *Phytochemistry*, **70**, 1017 (2009).
14. A. Petsalo, J. Jalonen and A. Tolonen, *J. Chromatogr. A*, **1112**, 224 (2006).
15. S.J. Bloor and S. Abrahams, *Phytochemistry*, **59**, 343 (2002).
16. L.O. Regasini, J.C. Vellosa, D.H. Silva, M. Furlan, O.M. de Oliveira, N.M. Khalil, I.L. Brunetti, M.C. Young, E.J. Barreiro and V.S. Bolzani, *Phytochemistry*, **69**, 1739 (2008).
17. C. Reinbothe, A. Springer, I. Samol and S. Reinbothe, *FEBS J.,* **276**, 4666 (2009).
18. I. Prost, S. Dhondt, G. Rothe, J. Vicente, M.J. Rodriguez, N. Kift, F. Carbonne, G. Griffiths, M.T. Esquerre-Tugaye, S. Rosahl, C. Castresana, M. Hamberg and J. Fournier, *Plant Physiol*., **139**, 1902 (2005).
19. G. Glauser, E. Grata, S. Rudaz and J.L. Wolfender, *Rapid Commun. Mass Spectrom.*, **22**, 3154 (2008).
20. M.A. Perez and M.A. Nussbaum, *J. Biomech.*, **36**, 1225 (2003).
21. M.K. Reid and K.L. Spencer, *Environ. Pollut.*, **157**, 2275 (2009).